



## **Finite-Blocklength Approximations for Noncoherent Rayleigh Block-Fading Channels**

Downloaded from: <https://research.chalmers.se>, 2025-04-26 05:29 UTC

Citation for the original published paper (version of record):

Lancho Serrano, A., Östman, J., Koch, T. et al (2019). Finite-Blocklength Approximations for Noncoherent Rayleigh Block-Fading Channels. Conference Record - Asilomar Conference on Signals, Systems and Computers, 2019-November: 815-819.  
<http://dx.doi.org/10.1109/IEEECONF44664.2019.9049072>

N.B. When citing this work, cite the original published paper.

© 2019 IEEE. Personal use of this material is permitted. Permission from IEEE must be obtained for all other uses, in any current or future media, including reprinting/republishing this material for advertising or promotional purposes, or reuse of any copyrighted component of this work in other works.

(article starts on next page)

# Finite-Blocklength Approximations for Noncoherent Rayleigh Block-Fading Channels

Alejandro Lancho\*, Johan Östman\*, Tobias Koch†, and Gonzalo Vazquez-Vilar†

\* Chalmers University of Technology, Gothenburg, Sweden.

† Universidad Carlos III de Madrid, Leganés, Spain, and Gregorio Marañón Health Research Institute, Madrid, Spain.

Emails: lancho@ieee.org, johanos@chalmers.se, koch@tsc.uc3m.es, gvazquez@ieee.org

**Abstract**—Several emerging wireless communication services and applications have stringent latency requirements, necessitating the transmission of short packets. To obtain performance benchmarks for short-packet wireless communications, it is crucial to study the maximum coding rate as a function of the blocklength, commonly called finite-blocklength analysis. A finite-blocklength analysis can be performed via nonasymptotic bounds or via refined asymptotic approximations. This paper reviews finite-blocklength approximations for the noncoherent Rayleigh block-fading channel. These approximations have negligible computational cost compared to the nonasymptotic bounds and are shown to be accurate for error probabilities as small as  $10^{-8}$  and SNRs down to 0 dB.

## I. INTRODUCTION

Traditional wireless communication technologies have focused on increasing the transmission rates without stringent latency constraints. Thus, the transmission of long packets is feasible and *capacity* and *outage capacity* provide accurate benchmarks for the throughput achievable in such systems. In contrast, current and upcoming generations of communication systems target, *inter alia*, the transmission of short packets at low rates [1]. Specifically, in ultra-reliable low-latency communications (URLLC), devices are expected to attain latencies below 1 ms and probabilities of error smaller than or equal to  $10^{-5}$ . In this scenario, capacity and outage capacity are too optimistic and a more refined characterization of the finite-blocklength performance is required.

The finite-blocklength performance can be characterized by means of nonasymptotic bounds. Polyanskiy *et al.* proposed the random-coding union (RCU) bound, the dependence-testing (DT) bound, and the meta-converse (MC) bound [2]. A relaxation of the RCU bound, based on the Chernoff bound, is the  $\text{RCU}_s$  bound [3, Th. 1]. Nonasymptotic bounds on the

maximum coding rate for noncoherent Rayleigh block-fading channels were studied in [4] for the single-antenna setting and in [5] for the multiple-input multiple-output (MIMO) setting.

Refined asymptotic analyses of the nonasymptotic bounds provide a complementary characterization of the finite-blocklength performance of communication systems. A so-called *error-exponent analysis* follows from fixing the coding rate and studying the exponential decay of the error probability as the blocklength tends to infinity. The resulting error exponent is referred to as the *reliability function* [6, Ch. 5]. Some results on the reliability function of fading channels can be found, e.g., in [7]–[10].

In contrast, a *dispersion* or *normal-approximation analysis* follows by fixing the error probability and studying the maximum coding rate as the blocklength tends to infinity [2]. Such an analysis has been carried out for fading channels, e.g., in [11]–[14]. Particularly relevant for this work is the high-SNR normal approximation for noncoherent single-antenna Rayleigh block-fading channels derived in [14].

A third approach to perform asymptotic analyses is the *saddlepoint method* [15, Ch. XVI]. The saddlepoint method yields an accurate approximation of the nonasymptotic bounds even where the error-exponent and normal approximation do not. This method has been applied to the RCU bound, the  $\text{RCU}_s$  bound, and the MC bound for some memoryless channels [16]–[18]. Saddlepoint approximations of the  $\text{RCU}_s$  bound and the MC bound for noncoherent single-antenna Rayleigh block-fading channels were derived in [9], [10].

In this paper, we present a summary of the existing nonasymptotic bounds and approximations for noncoherent single-antenna Rayleigh block-fading channels. We assess the accuracy of the approximations by means of numerical examples and discuss their computational complexity.

## II. RAYLEIGH BLOCK-FADING CHANNEL

We consider a single-antenna Rayleigh block-fading channel with coherence interval  $T$ . For this channel model, the input-output relation within the  $\ell$ -th coherence interval is given by

$$\mathbf{Y}_\ell = H_\ell \mathbf{X}_\ell + \mathbf{W}_\ell \quad (1)$$

where  $\mathbf{X}_\ell$  and  $\mathbf{Y}_\ell$  are  $T$ -dimensional, complex-valued, random vectors containing the input and output signals, respectively;  $\mathbf{W}_\ell$  is the additive noise with i.i.d., circularly-symmetric,

A. Lancho has received funding from the European Research Council (ERC) under the European Union’s Horizon 2020 research and innovation programme (grant agreement number 714161) and from the Swedish Research Council under grant 2016-03293. J. Östman has been supported by the Swedish Research Council under grants 2014-6066 and 2016-03293. T. Koch has received funding from the European Research Council (ERC) under the European Union’s Horizon 2020 research and innovation programme (grant agreement number 714161) and from the Spanish Ministerio de Economía y Competitividad under grants RYC-2014-16332 and TEC2016-78434-C3-3-R (AEI/FEDER, EU). G. Vazquez-Vilar has received funding from the European Research Council (ERC) under the European Union’s Horizon 2020 research and innovation programme (grant agreement number 714161) and from the Spanish Ministerio de Economía y Competitividad under grant TEC2016-78434-C3-3-R (AEI/FEDER, EU).

complex Gaussian entries; and  $H_\ell$  is a circularly-symmetric complex Gaussian random variable. We assume that  $H_\ell$  and  $\mathbf{W}_\ell$  are mutually independent and take on independent realizations over successive coherence intervals. We consider a noncoherent setting where transmitter and receiver are aware of the distribution of  $H_\ell$  but not of its realization.

We next introduce the notion of a channel code. We shall restrict ourselves to codes of blocklength  $n = LT$ , where  $L$  denotes the number of coherence intervals of length  $T$  needed to transmit the entire codeword.

An  $(M, L, T, \epsilon, \rho)$ -code for the channel (1) consists of:

- 1) An encoder  $f: \{1, \dots, M\} \rightarrow \mathbb{C}^{LT}$  that maps the message  $A$ , which is uniformly distributed on  $\{1, \dots, M\}$ , to a codeword  $\mathbf{X}^L = [\mathbf{X}_1, \dots, \mathbf{X}_L] = f(A)$  satisfying<sup>1</sup>

$$\|\mathbf{X}_\ell\|^2 = T\rho, \quad \ell = 1, \dots, L. \quad (2)$$

- 2) A decoder  $g: \mathbb{C}^{LT} \rightarrow \{1, \dots, M\}$  satisfying

$$\mathbb{P}[g(\mathbf{Y}^L) \neq A] \leq \epsilon \quad (3)$$

where  $\mathbf{Y}^L = [\mathbf{Y}_1, \dots, \mathbf{Y}_L]$  is the channel output induced by the transmitted codeword  $\mathbf{X}^L = f(A)$ .

The *maximum coding rate* and *minimum error probability* are respectively defined as

$$R^*(L, T, \epsilon, \rho) \triangleq \sup \left\{ \frac{\log(M)}{LT} : \exists (M, L, T, \epsilon, \rho)\text{-code} \right\} \quad (4)$$

$$\epsilon^*(L, T, R, \rho) \triangleq \inf \{ \epsilon : \exists (2^{LTR}, L, T, \epsilon, \rho)\text{-code} \}. \quad (5)$$

Note that upper (lower) bounds on  $\epsilon^*(L, T, R, \rho)$  can be turned into lower (upper) bounds on  $R^*(L, T, \epsilon, \rho)$  and *vice versa*.

### III. NONASYMPTOTIC BOUNDS

Throughout the paper, we evaluate the achievability bounds for the capacity-achieving input distribution, under which the inputs are of the form  $\mathbf{X}^L = \sqrt{T\rho}\mathbf{U}^L$  (where the components of  $\mathbf{U}^L = [\mathbf{U}_1, \dots, \mathbf{U}_L]$  are i.i.d. and uniformly distributed on the unit sphere in  $\mathbb{C}^T$ ). We denote by  $\bar{\mathbb{P}}_{\mathbf{X}}$  the distribution of  $\mathbf{X}_\ell = \sqrt{T\rho}\mathbf{U}_\ell$ . We define the *generalized information density* as

$$i_s(\mathbf{x}_\ell; \mathbf{y}_\ell) \triangleq \log \frac{\mathbb{P}_{\mathbf{Y}_\ell|\mathbf{X}_\ell}(\mathbf{y}_\ell|\mathbf{x}_\ell)^s}{\bar{\mathbb{P}}_{\mathbf{Y}_\ell}^s(\mathbf{y}_\ell)}, \quad s > 0 \quad (6)$$

$$\bar{\mathbb{P}}_{\mathbf{Y}_\ell}^s(\mathbf{y}_\ell) \triangleq \int \mathbb{P}_{\mathbf{Y}_\ell|\mathbf{X}_\ell}(\mathbf{y}_\ell|\mathbf{x}_\ell)^s d\bar{\mathbb{P}}_{\mathbf{X}}(\mathbf{x}_\ell), \quad s > 0. \quad (7)$$

It can be shown that  $i_s(\mathbf{X}_\ell; \mathbf{Y}_\ell)$  depends on  $\mathbf{X}_\ell$  only via  $\|\mathbf{X}_\ell\|^2 = T\rho$ . Thus, conditioned on  $\|\mathbf{X}_\ell\|^2 = T\rho$ , [10]

$$\begin{aligned} i_s(\mathbf{X}_\ell; \mathbf{Y}_\ell) &\stackrel{\mathcal{L}}{=} (T-1) \log(st\rho) - \log \Gamma(T) - s \frac{T\rho Z_{2,\ell}}{1+T\rho} \\ &+ (T-1) \log \left( \frac{(1+T\rho)Z_{1,\ell} + Z_{2,\ell}}{1+T\rho} \right) \\ &- \log \tilde{\gamma} \left( T-1, s \frac{T\rho((1+T\rho)Z_{1,\ell} + Z_{2,\ell})}{1+T\rho} \right) \end{aligned} \quad (8)$$

<sup>1</sup>While in the information theory literature it is more common to impose a power constraint per codeword  $\mathbf{X}^L$ , practical systems typically require a per-coherence-interval constraint. Although it may be preferable to impose (2) with inequality, in this paper we restrict ourselves to using maximum power. For the high-SNR normal approximation presented in [14], this turns out to be the optimal case.

where we use “ $\stackrel{\mathcal{L}}{=}$ ” to denote equality in distribution, and where  $\Gamma(\cdot)$  and  $\tilde{\gamma}(\cdot)$  denote the gamma function and the regularized lower incomplete gamma function, respectively. In (8),  $\{Z_{1,\ell}\}_{\ell=1}^L$  are i.i.d. gamma(1, 1)-distributed random variables, and  $\{Z_{2,\ell}\}_{\ell=1}^L$  are i.i.d. gamma( $T-1$ , 1)-distributed random variables. For brevity, we let  $i_{\ell,s}(\rho) \triangleq i_s(\mathbf{X}_\ell; \mathbf{Y}_\ell)$ , and we define the expectation and variance of  $i_{\ell,s}(\rho)$  by  $I_s(\rho) \triangleq \mathbb{E}[i_{\ell,s}(\rho)]$  and  $V_s(\rho) \triangleq \text{Var}[i_{\ell,s}(\rho)]$ .

The RCU<sub>s</sub> bound [3, Th. 1] states that, for every  $s > 0$ ,

$$\epsilon^*(L, T, R, \rho) \leq \mathbb{P} \left[ \sum_{\ell=1}^L i_{\ell,s}(\rho) \leq LTR - \log(\theta) \right] \quad (9)$$

where  $\theta$  is uniformly distributed on the interval  $[0, 1]$ .

For any  $s > 0$ , we define the auxiliary output probability density function (pdf)

$$q_{\mathbf{Y}_\ell}^s(\mathbf{y}_\ell) \triangleq \frac{1}{\mu(s)} \left( \int \mathbb{P}_{\mathbf{Y}_\ell|\mathbf{X}_\ell}(\mathbf{y}_\ell|\mathbf{x}_\ell)^s d\bar{\mathbb{P}}_{\mathbf{X}}(\mathbf{x}_\ell) \right)^{1/s} \quad (10)$$

where  $\mu(s)$  is a normalizing factor. A lower bound on  $\epsilon^*(L, T, R, \rho)$  follows by evaluating the MC bound [2, Th.31] for the auxiliary pdf  $q_{\mathbf{Y}_\ell}^s$  and using [2, Eq. (102)]. We then obtain that, for every  $\xi > 0$  and  $s > 0$ ,

$$\begin{aligned} \epsilon^*(L, T, R, \rho) &\geq \mathbb{P} \left[ \sum_{\ell=1}^L i_{\ell,s}(\rho) \leq s \log \xi - sL \log \mu(s) \right] - \xi e^{-LTR}. \end{aligned} \quad (11)$$

For  $s = 1$ , both  $\bar{\mathbb{P}}_{\mathbf{Y}_\ell}^s$  and  $q_{\mathbf{Y}_\ell}^s$  coincide with the capacity-achieving output distribution, in which case (9) and (11) recover the DT and MC bounds derived in [2]. For brevity, we write  $i_\ell(\rho) \triangleq i_{\ell,1}(\rho)$ ,  $V(\rho) \triangleq V_1(\rho)$ , and  $C(\rho) \triangleq I_1(\rho)$ .<sup>2</sup>

We shall see in Section VII that the nonasymptotic bounds (9) and (11) precisely characterize the triple  $(R, \epsilon, n)$ . However, their high computational complexity hinders their practical application for URLLC scenarios. In the following, we present asymptotic approximations of these bounds that are easier to compute.

### IV. ERROR EXPONENT APPROXIMATION

We define the *reliability function* as [6]

$$E_r(T, R, \rho) \triangleq \lim_{L \rightarrow \infty} -\frac{1}{L} \log \epsilon^*(L, T, R, \rho). \quad (12)$$

Let  $\tau \mapsto \kappa_{\rho,s}(\tau)$  denote the cumulant generating function (CGF) of the zero-mean random variable  $I_s(\rho) - i_{\ell,s}(\rho)$ , i.e.,

$$\kappa_{\rho,s}(\tau) = \log \mathbb{E} \left[ e^{\tau(I_s(\rho) - i_{\ell,s}(\rho))} \right] \quad (13)$$

and let  $\kappa'_{\rho,s}$ ,  $\kappa''_{\rho,s}$ , and  $\kappa'''_{\rho,s}$  denote the first three derivatives of  $\kappa_{\rho,s}$ . The *critical rate* of the channel is defined as [6, Eq. (5.6.30)]

$$R_s^{\text{cr}}(\rho) \triangleq \frac{1}{T} (I_s(\rho) - \kappa'_{\rho,s}(1)). \quad (14)$$

<sup>2</sup>The USTM input distribution is capacity achieving for the power constraint considered in (2). Hence,  $I_1(\rho)$  coincides with the capacity of the channel.

For rates above  $R_s^{\text{cr}}(\rho)$ , the error exponents of (9) and (11) coincide and, setting  $s = \frac{1}{1+\tau}$ , we obtain the following result.

*Theorem 1 (Error exponent approximation):* Assume that  $R_{1/2}^{\text{cr}}(\rho) \leq R \leq C(\rho)$ , and let

$$R(\tau) = \frac{1}{T} \left( I_{\frac{1}{1+\tau}}(\rho) - \kappa'_{\rho, \frac{1}{1+\tau}}(\tau) \right) \quad (15)$$

$$E_r(\tau) = \tau \kappa'_{\rho, \frac{1}{1+\tau}}(\tau) - \kappa_{\rho, \frac{1}{1+\tau}}(\tau) \quad (16)$$

where  $\tau$  is the solution of  $R(\tau) = R$ . Then,

$$\epsilon^*(L, T, R, \rho) = e^{-L[E_r(\tau) + o_{\tau, L}(1)]} \quad (17)$$

where  $o_{\tau, L}(1)$  comprises terms that depend on  $(\tau, L)$ , are uniform in  $\rho$ , and vanish as  $L \rightarrow \infty$ .

*Proof:* See [19, Sec. 6.4]. ■

## V. NORMAL APPROXIMATIONS

An application of the central limit theorem (CLT) shows that we can approximate the tail probabilities in (9) and (11) by those of a normal distribution with a certain mean and variance. The resulting expression is the so-called normal approximation, which is presented next.

*Theorem 2 (Normal approximation):* The maximum coding rate in a single-antenna Rayleigh block-fading channel satisfies

$$R^*(L, T, \epsilon, \rho) = \frac{C(\rho)}{T} - \sqrt{\frac{V(\rho)}{LT^2}} Q^{-1}(\epsilon) + \mathcal{O}_L\left(\frac{\log L}{L}\right) \quad (18)$$

where  $Q^{-1}(\cdot)$  denotes the inverse of the Gaussian  $Q$ -function, and  $\mathcal{O}_L((\log L)/L)$  collects terms of order  $(\log L)/L$  that are uniform in  $\rho$ .

*Proof:* See [19, Sec. 6.3]. ■

The channel capacity  $C(\rho)$  and channel dispersion  $V(\rho)$  have no closed-form expression and must be evaluated numerically. A closed-form high-SNR normal approximation [14, Th. 2] can be obtained from (18) by using that [14, Eqs. (38)–(39)]

$$\begin{aligned} C(\rho) &= (T-1) \log(T\rho) - \log \Gamma(T) \\ &\quad - (T-1) \left[ \log(1+T\rho) + \frac{T\rho}{1+T\rho} - \psi(T-1) \right] \\ &\quad + {}_2F_1\left(1, T-1; T; \frac{T\rho}{1+T\rho}\right) + o_\rho(1) \end{aligned} \quad (19)$$

$$V(\rho) = (T-1)^2 \frac{\pi^2}{6} + (T-1) + o_\rho(1) \quad (20)$$

where  $o_\rho(1)$  comprises terms that are uniform in  $L$  and vanish as  $\rho \rightarrow \infty$ . In (19),  $\psi(\cdot)$  denotes the digamma function and  ${}_2F_1(\cdot, \cdot; \cdot; \cdot)$  denotes the Gauss hypergeometric function.

## VI. SADDLEPOINT APPROXIMATIONS

Similar to the CLT, the saddlepoint method [15, Ch. XVI] can be used to estimate tail probabilities. This method first applies an exponential tilting to the distribution of the random variable inside the tail probability, followed by a CLT-based approximation over the tilted distribution.

Before we present the saddlepoint expansions of the nonasymptotic bounds (9) and (11), we first discuss the region

of convergence of the moment generating function (MGF) of  $I_s(\rho) - i_{\ell, s}(\rho)$ . Let

$$m_{\rho, s}(\tau) \triangleq \mathbb{E} \left[ e^{\tau(I_s(\rho) - i_{\ell, s}(\rho))} \right] \quad (21)$$

and let  $m_{\rho, s}^{(k)}$  denote the  $k$ -th derivative of  $m_{\rho, s}$ . It can be shown that [19, Lemma 4.2]

$$\sup_{(\tau, \rho, s) \in \mathcal{S}} m_{\rho, s}^{(k)}(\tau) < \infty \quad (22)$$

for every nonnegative integer  $k$ , where

$$\mathcal{S} \triangleq \{(\tau, \rho, s) \in \mathbb{R}^3 : \tau \in [a, b], \rho \in [\underline{\rho}, \bar{\rho}], s \in [\underline{s}, \bar{s}]\} \quad (23)$$

for some arbitrary  $0 < \underline{s} < \bar{s}$ ,  $0 < \underline{\rho} < \bar{\rho}$ , and  $0 < a < b < \min\{\frac{T}{T-1}, \frac{1+T\bar{\rho}}{T\rho s}\}$ . Thus, the set  $\mathcal{S}$  is in the region of convergence of  $m_{\rho, s}$ , and we obtain the following results.

*Theorem 3 (Saddlepoint Expansion  $RCU_s$ ):* The coding rate  $R$  and minimum error probability  $\epsilon^*$  can be parametrized by  $(\tau, \rho, s) \in \mathcal{S}$  as

$$R(\tau, s) = \frac{1}{T} (I_s(\rho) - \kappa'_{\rho, s}(\tau)) \quad (24)$$

$$\begin{aligned} \epsilon^*(\tau, s) &\leq e^{L[\kappa_{\rho, s}(\tau) - \tau \kappa'_{\rho, s}(\tau)]} \\ &\quad \times \left[ f_{\rho, s}(\tau, \tau) + f_{\rho, s}(1-\tau, \tau) + \frac{\hat{K}_{\rho, s}(\tau)}{\sqrt{L}} + o_L\left(\frac{1}{\sqrt{L}}\right) \right] \end{aligned} \quad (25)$$

where

$$f_{\rho, s}(u, \tau) \triangleq e^{n \frac{u^2}{2} \kappa''_{\rho, s}(\tau)} Q\left(u \sqrt{n \kappa''_{\rho, s}(\tau)}\right) \quad (26)$$

$$\hat{K}_{\rho, s}(\tau) \triangleq \frac{2}{\sqrt{2\pi}} \frac{\kappa'''_{\rho, s}(\tau)}{6 \kappa''_{\rho, s}(\tau)^{3/2}} \quad (27)$$

and  $o_L(1/\sqrt{L})$  comprises terms that vanish faster than  $1/\sqrt{L}$  and are uniform in  $(\tau, s, \rho)$ .

*Proof:* See [10, Th. 3]. ■

*Remark 1:* The set  $\mathcal{S}$  with  $\bar{s} = 1$  includes  $0 \leq \tau < 1$ . In this case, the identity (24) characterizes all rates  $R$  between the critical rate (14) and  $I_s(\rho)$ . Solving (24) for  $\tau$ , we thus obtain from Theorem 3 an upper bound on  $\epsilon^*(L, T, R, \rho)$  as a function of the rate  $R \in (R_s^{\text{cr}}(\rho), I_s(\rho))$ ,  $s \in (0, 1]$ .

*Theorem 4 (Saddlepoint Expansion MC):* For every rate  $R$  and  $(\tau, \rho, s) \in \mathcal{S}$

$$\begin{aligned} \epsilon^*(L, T, R, \rho) &\geq -e^{L[\log \mu(s) + \frac{1}{s} I_s(\rho) - \frac{\kappa'_{\rho, s}(\tau)}{s} - TR]} \\ &\quad + e^{L[\kappa_{\rho, s}(\tau) - \tau \kappa'_{\rho, s}(\tau)]} \left[ f_{\rho, s}(\tau, \tau) + \frac{K_{\rho, s}(\tau, L)}{\sqrt{L}} + o_L\left(\frac{1}{\sqrt{L}}\right) \right] \end{aligned} \quad (28)$$

where  $f_{\rho, s}(\cdot, \cdot)$  is defined in (26),  $K_{\rho, s}(\cdot, \cdot)$  is given by

$$\begin{aligned} K_{\rho, s}(\tau, n) &\triangleq \frac{\kappa'''_{\rho, s}(\tau)}{6 \kappa''_{\rho, s}(\tau)^{3/2}} \left( -\frac{1}{\sqrt{2\pi}} + \frac{\tau^2 \kappa''_{\rho, s}(\tau) n}{\sqrt{2\pi}} \right. \\ &\quad \left. - \tau^3 \kappa''_{\rho, s}(\tau)^{3/2} n^{3/2} f_{\rho, s}(\tau, \tau) \right) \end{aligned} \quad (29)$$

and  $o_L(1/\sqrt{L})$  comprises terms that vanish faster than  $1/\sqrt{L}$  and are uniform in  $(\tau, s, \rho)$ .

*Proof:* See [10, Th. 4]. ■

The saddlepoint expansions (25) and (28) can be written as an exponential term times a subexponential factor. The exponential terms of both expansions coincide for rates above the critical rate and yield the reliability function (12). We next present the corresponding subexponential factors.

*Theorem 5:* Let  $\underline{\rho} \leq \rho \leq \bar{\rho}$  and  $\underline{\tau} < \tau < \bar{\tau}$  for some arbitrary  $0 < \underline{\rho} < \bar{\rho}$  and  $0 < \underline{\tau} < \bar{\tau} < 1$ , and set  $s_\tau \triangleq 1/(1+\tau)$ . The coding rate  $R$  and the minimum error probability  $\epsilon^*$  can be parametrized by  $\tau \in (\underline{\tau}, \bar{\tau})$  as

$$R(\tau) = \frac{1}{T} (I_{s_\tau}(\rho) - \kappa'_{\rho, s_\tau}(\tau)) \quad (30)$$

$$\underline{A}_\rho(\tau) \leq \epsilon^*(L, T, R, \rho) e^{-L[\kappa_{\rho, s_\tau}(\tau) - \tau \kappa'_{\rho, s_\tau}(\tau)]} \leq \bar{A}_\rho(\tau) \quad (31)$$

where

$$\bar{A}_\rho(\tau) \triangleq \frac{1}{\sqrt{2\pi L \tau^2 \kappa''_{\rho, s_\tau}(\tau)}} + \frac{|\hat{K}_{\rho, s_\tau}(\tau)|}{\sqrt{L}} + \frac{1}{\sqrt{2\pi L (1-\tau)^2 \kappa''_{\rho, s_\tau}(\tau)}} + o_L\left(\frac{1}{\sqrt{L}}\right) \quad (32)$$

$$\underline{A}_\rho(\tau) \triangleq \frac{s_\tau^{\frac{1}{2\tau}}}{\tau (2\pi L \kappa''_{\rho, s_\tau}(\tau))^{\frac{1}{2s_\tau}}} + o_L\left(\frac{1}{L^{2s_\tau}}\right). \quad (33)$$

The little- $o$  term in (32) vanishes faster than  $1/\sqrt{L}$  uniformly in  $\rho$  and  $\tau$ . The little- $o$  term in (33) vanishes faster than  $1/L^{1/2s_\tau}$  and is uniform in  $\rho$  (for every given  $\tau$ ) [10].

*Proof:* See [19, Th. 6.6]. ■

## VII. DISCUSSION

### A. Numerical Comparison

We obtain approximations of the RCU<sub>s</sub> and MC bounds by disregarding the error terms in Theorems 1–5. Approximations of the RCU<sub>s</sub> bound are plotted in red and approximations of the MC bound are plotted in blue. Straight lines (“saddlepoint”) depict the saddlepoint approximations (25) and (28), and dashed lines (“pref+EE”) depict (31). We further plot the nonasymptotic bounds (9) and (11) with dots. Finally, we plot the normal approximation (18) (“NA”), the high-SNR normal approximation [14, Th. 2] (“high-SNR-NA”), and the error-exponent approximation (17) (“EEA”).

In Fig. 1, we study  $R^*(L, T, \epsilon, \rho)$  as a function of  $L$  for  $n = 168$  (hence  $T$  is inversely proportional to  $L$ ),  $\epsilon = 10^{-5}$ , and SNR values 0 dB and 10 dB. Observe that the approximations (25), (28), and (31) are almost indistinguishable from the nonasymptotic bounds. Further observe that the normal approximation “NA” is accurate for 10 dB and  $L > 10$ , but is loose for 0 dB. In contrast, the error exponent approximation “EEA” is loose for 10 dB, but accurate for 0 dB.

In Fig. 2, we study  $R^*(L, T, \epsilon, \rho)$  as a function of  $\epsilon$  for  $n = 168$  ( $T = 12$  and  $L = 14$ ) and SNR values 6 dB and 0 dB. We also show the critical rate  $R_{1/2}^{\text{cr}}(0)$  for  $\rho = 0$  dB. Observe that the approximations (25), (28), and (31) are almost indistinguishable from the nonasymptotic bounds. Further observe how the normal approximation “NA” becomes accurate for

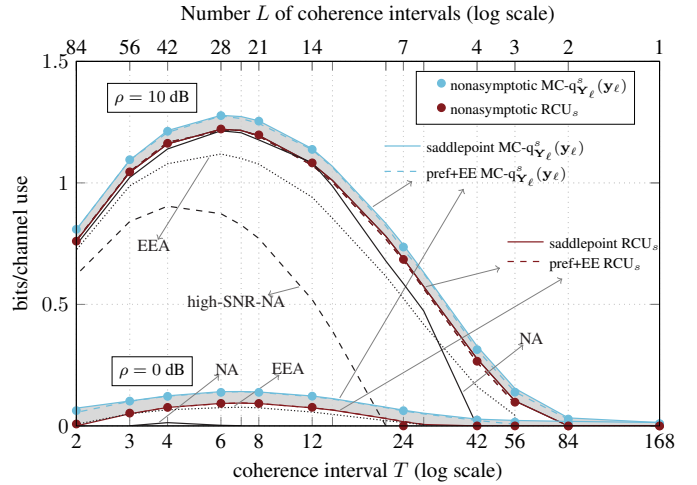


Fig. 1: Bounds on  $R^*(L, T, \epsilon, \rho)$  for  $n = 168$ ,  $\epsilon = 10^{-5}$ ,  $\rho = \{0, 10\}$  dB.

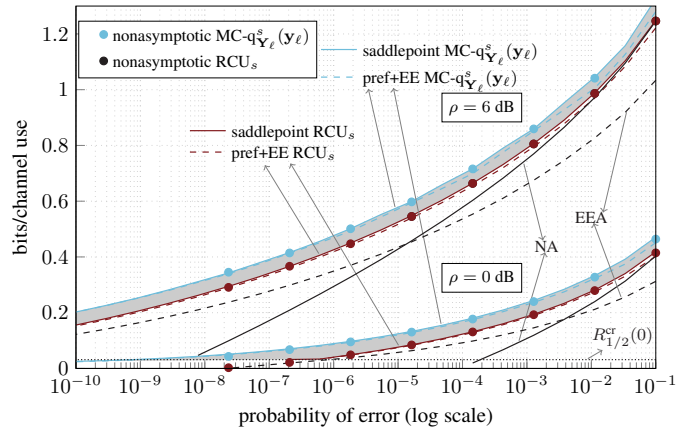


Fig. 2: Bounds on  $R^*(L, T, \epsilon, \rho)$  for  $n = 168$ ,  $T = 12$ ,  $\rho = \{0, 6\}$  dB.

large error probabilities, whereas the error exponent approximation “EEA” becomes accurate for small error probabilities.

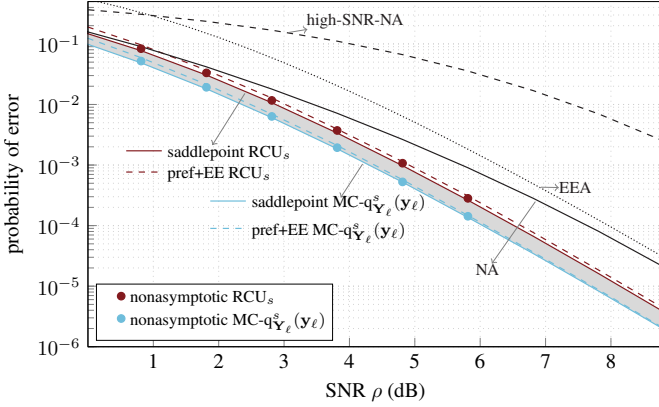
In Fig. 3, we study  $\epsilon^*(L, T, R, \rho)$  as a function of the SNR  $\rho$  for  $n = 168$  ( $T = 24$  and  $L = 7$ ) and  $R = 0.48$ . Observe that in this scenario the approximations (25), (28), and (31) are the only accurate approximations of the nonasymptotic bounds.

### B. Complexity vs. Accuracy

Table I summarizes the computational complexity and accuracy of the bounds and approximations presented in this paper. Specifically, we denote by  $N$  the cost of numerically evaluating a one-dimensional integral and by  $K$  the cost of optimizing over an auxiliary parameter. We then provide a rough estimate of the complexity of the presented bounds and approximations in terms of  $N$  and  $K$ . For example, the nonasymptotic bounds require the evaluation of the distribution function of  $\sum_{\ell=1}^L i_{\ell, s}(\rho)$  which, for the RCU<sub>s</sub> bound corresponds to an  $(2L+1)$ -dimensional integral (over  $\{Z_{1, \ell}\}_{\ell=1}^L$ ,  $\{Z_{2, \ell}\}_{\ell=1}^L$ , and  $\theta$ ) and the optimization over  $s$  and, for the MC bound, corresponds to an  $(2L)$ -dimensional integral and the optimization over  $s$  and  $\xi$ . The numerical evaluation of an  $L$ -dimensional integral has a complexity of roughly  $N^L$ , hence the overall complexity is  $KN^{2L+1}$  for the RCU<sub>s</sub> bound and  $K^2N^{2L}$  for the MC bound. The approximations (25), (28),

TABLE I: Complexity and accuracy of the analyzed bounds and approximations.

Bound/Approximation	Complexity	Accuracy
<b>Nonasymptotic bounds</b>	RCU <sub>s</sub> : $KN^{2L+1}$ (optimization over $s$ ) MC: $K^2N^{2L}$ (optimization over $s, \xi$ )	Exact. Computable for moderate values of $L$ and $\epsilon$ . For example, for $L = 14$ , computable for $\epsilon > 10^{-8}$ . For $L = 84$ , computable for $\epsilon > 10^{-5}$ .
<b>Saddlepoint approximation</b>	$5K^2N^2$ (optimization over $\tau, s$ )	Almost indistinguishable from nonasymptotic bounds over the entire range of system parameters.
<b>Prefactor-and-error-exponent approximation</b>	$5KN^2$ (optimization over $\tau$ )	Almost as accurate as saddlepoint approximation and easier to interpret analytically.
<b>Error-exponent approximation</b>	$3KN^2$ (optimization over $\tau$ )	Accurate for small values of $\rho$ and $\epsilon$ . For example, for $\rho = 6$ dB, accurate for $\epsilon < 10^{-7}$ . For $\rho = 0$ dB, accurate for $\epsilon < 10^{-4}$ .
<b>Normal approximation</b>	$2N^2$ (no optimization)	Accurate for large values of $\rho$ and $\epsilon$ . For example, for $\rho = 6$ dB, accurate for $\epsilon > 10^{-3}$ . For $\rho = 0$ dB, accurate for $\epsilon > 10^{-2}$ .
<b>High-SNR normal approximation</b>	available in closed form	Accurate for $\rho \geq 15$ dB and $L \geq 10$ and large values of $\epsilon$ [14].


 Fig. 3: Bounds on  $\epsilon^*(L, T, R, \rho)$  for  $n = 168$ ,  $T = 24$ ,  $R = 0.48$ .

and (31) depend on  $I_s(\rho)$ ,  $\kappa_{\rho,s}$ ,  $\kappa'_{\rho,s}$ ,  $\kappa''_{\rho,s}$ , and  $\kappa'''_{\rho,s}$ , so they can be obtained by solving 5 two-dimensional integrals and by optimizing over  $\tau$  and  $s$ . The error-exponent approximation (17) can be obtained by evaluating  $I_{s\tau}(\rho)$ ,  $\kappa_{\rho,s\tau}$ , and  $\kappa'_{\rho,s\tau}$ , which corresponds to the evaluation of 3 two-dimensional integrals and by optimizing over  $\tau$ . The normal approximation (18) can be obtained by evaluating  $C(\rho)$  and  $V(\rho)$ , which corresponds to the evaluation of 2 two-dimensional integrals. The high-SNR normal approximation is available in closed form.

Observe that the computational complexity of the nonasymptotic bounds grows exponentially in  $L$ , whereas the presented approximations have a computational complexity that is independent of  $L$ . This is a significant reduction in computational cost, especially if  $L$  is large. The saddlepoint approximations, as observed in Section VII-A, exhibit almost the same accuracy as the nonasymptotic bounds over a large range of system parameters at a negligible computational cost. The normal approximations and the error-exponent approximation have an even lower computational complexity, but they are only accurate in a limited range of system parameters.

In summary, the normal approximations and the error-exponent approximation yield accurate characterizations of the maximum coding rate only for certain ranges of the system parameters. In contrast, the saddlepoint approximations arise as easy-to-compute alternatives to the nonasymptotic bounds when one wishes to characterize the maximum coding rate for a large range of system parameters or for system parameters where neither normal approximations nor error-exponent approximation are accurate.

## REFERENCES

- [1] G. Durisi, T. Koch, and P. Popovski, "Towards massive, ultra-reliable, and low-latency wireless communication with short packets," *Proc. IEEE*, vol. 104, no. 9, pp. 1711–1726, Sep. 2016.
- [2] Y. Polyanskiy, H. V. Poor, and S. Verdú, "Channel coding rate in the finite blocklength regime," *IEEE Trans. Inf. Theory*, vol. 56, no. 5, pp. 2307–2359, May 2010.
- [3] A. Martinez and A. Guillén i Fàbregas, "Saddlepoint approximation of random-coding bounds," in *Proc. Inf. Theory Applicat. Workshop (ITA)*, La Jolla, CA, USA, Feb. 2011.
- [4] W. Yang, G. Durisi, T. Koch, and Y. Polyanskiy, "Diversity versus channel knowledge at finite block-length," in *Proc. IEEE Inf. Theory Workshop (ITW)*, Lausanne, Switzerland, Sep. 2012, pp. 572–576.
- [5] G. Durisi, T. Koch, J. Östman, Y. Polyanskiy, and W. Yang, "Short-packet communications over multiple-antenna Rayleigh-fading channels," *IEEE Trans. on Commun.*, vol. 64, no. 2, pp. 618–629, Feb. 2016.
- [6] R. G. Gallager, *Information Theory and Reliable Communication*, 1st ed. New York, NY, USA: John Wiley & Sons, 1968.
- [7] I. Abou-Faycal and B. M. Hochwald, "Coding requirements for multiple-antenna channels with unknown Rayleigh fading," Bell Labs., Lucent Technologies, Tech. Rep., 1999.
- [8] J. Östman, G. Durisi, E. G. Ström, M. C. Coşkun, and G. Liva, "Short packets over block-memoryless fading channels: Pilot-assisted or noncoherent transmission?" *IEEE Trans. Commun.*, vol. 67, no. 2, pp. 1521–1536, Feb. 2019.
- [9] A. Lancho, J. Östman, G. Durisi, T. Koch, and G. Vazquez-Vilar, "Saddlepoint approximations for noncoherent Rayleigh block-fading channels," in *Proc. IEEE Int. Symp. Inf. Theory (ISIT)*, Paris, France, Jul. 2019.
- [10] —, "Saddlepoint approximations for short-packet wireless communications," arXiv:1904.10442 [cs.IT], Sep. 2019.
- [11] Y. Polyanskiy and S. Verdú, "Scalar coherent fading channel: Dispersion analysis," in *Proc. IEEE Int. Symp. Inf. Theory (ISIT)*, St. Petersburg, Russia, Jul. 2011, pp. 2959–2963.
- [12] A. Collins and Y. Polyanskiy, "Coherent multiple-antenna block-fading channels at finite blocklength," *IEEE Trans. Inf. Theory*, vol. 65, no. 1, pp. 380–405, Jan. 2019.
- [13] W. Yang, G. Durisi, T. Koch, and Y. Polyanskiy, "Quasi-static multiple-antenna fading channels at finite blocklength," *IEEE Trans. Inf. Theory*, vol. 60, no. 7, pp. 4232–4265, Jul. 2014.
- [14] A. Lancho, T. Koch, and G. Durisi, "On single-antenna Rayleigh block-fading channels at finite blocklength," *IEEE Trans. Inf. Theory*, Oct. 2019, to be published.
- [15] W. Feller, *An Introduction To Probability Theory And Its Applications*, 2nd ed. New York, NY, USA: Wiley, 1971, vol. II.
- [16] J. Scarlett, A. Martinez, and A. Guillén i Fàbregas, "Mismatched decoding: Error exponents, second-order rates and saddlepoint approximations," *IEEE Trans. Inf. Theory*, vol. 60, no. 5, pp. 2647–2666, May 2014.
- [17] J. Font-Segura, G. Vazquez-Vilar, A. Guillén i Fàbregas, and A. Lancho, "Saddlepoint approximations in random coding," in *Proc. Conference on Inf. Sci. and Sys. (CISS)*, Princeton, NJ, USA, Mar. 2018.
- [18] G. Vazquez-Vilar, A. Guillén i Fàbregas, T. Koch, and A. Lancho, "Saddlepoint approximation of the error probability of binary hypothesis testing," in *Proc. IEEE Int. Symp. Inf. Theory (ISIT)*, Vail, CO, USA, Jun. 2018.
- [19] A. Lancho, "Fundamental limits of short-packet wireless communications," Ph.D. dissertation, Universidad Carlos III de Madrid, Jun. 2019.